Storage efficiency of probe pulses in an electromagnetically-induced-transparency medium

Rui Zhang[1,2] and Xiang-Bin Wang[1,2,3,*]

[1]*State Key Laboratory of Low Dimensional Quantum Physics, Department of Physics, Tsinghua University, Beijing 100084, People's Republic of China*

[2]*Synergetic Innovation Center of Quantum Information and Quantum Physics, University of Science and Technology of China, Hefei, Anhui 230026, People's Republic of China*

[3]*Jinan Institute of Quantum Technology, SAICT, Jinan 250101, People's Republic of China*

(Received 18 July 2016; published 27 December 2016)

We have studied light storage in an electromagnetically-induced-transparency medium. The total storage efficiency for the probe pulse has been presented, with and without adiabatic approximation. Storage with different control parameters has been discussed and the influences on storage efficiency have been addressed. We have found that good efficiency can be achieved by using easily controlled wave shapes for the control field.

DOI: 10.1103/PhysRevA.94.063856

I. INTRODUCTION

As one of the fundamental building blocks in quantum networks, quantum memory (storage and retrieval of a photon pulse) plays a crucial role in quantum-information processing [1–3]. Motivated by this, a lot of theoretical and experimental research has been conducted in recent years [4–10]. In the study of quantum memory, one common realization for the storage and retrieval of a photon pulse is a cold atomic ensemble. By using the electromagnetically-induced-transparency (EIT) effect, high-quality storage and retrieval of a photon pulse can be achieved. For example, in the experiment of Ref. [11], the photon polarization state can be stored in the cold atomic medium as two magnetic-field-insensitive spin waves. For another example, by applying the spin echo technique, one can realize long-lived quantum memory at the single-photon level [12].

As we know, compared with a long pulse, a short pulse is much easier to produce in practice and its energy is more concentrated [13–16]. So there are many advantages to use short probe pulses in quantum computation and quantum communication. Encouraged by this, the utilization of EIT systems with short probe pulses have attracted wide attention in the implementation of both quantum gates and quantum memories. In Ref. [17], Lene Hau *et al.* first completed the slow-light experiment based on the EIT effect, and reported the first measurement of giant Kerr nonlinearities produced by EIT. Thus, one can make use of this strong nonlinear interaction to achieve logic gates, and also use it in gate-based quantum computation. One proposal is to realize the quantum gates with optical fields acquiring a π rad cross-phase shift [18,19]. To achieve high fidelity and large conditional phase shift simultaneously (there is a tradeoff between these two quantities in the stationary regime), in their papers [18,19], the authors applied the nonlinear properties of the EIT systems. In the full quantum limit and transient regime, a two-qubit quantum phase gate with high fidelity and fast operation has been addressed first. In another proposal, the nonlinear phase shift in the probe field has been detected [20]. Such a phase shift is related to a short pulse at the single-photon level. Moreover, recently, many researchers have made use of the concentrated energy in a short pulse to realize the giant cross-phase modulation, see Refs. [13,14,20]. In Ref. [15], the authors realized the quantum memory for a subnanosecond short light pulse. Utilization of a temporal short pulse can achieve a higher data rate, which is very important in quantum communication, and enable the quantum information to be processed at a high speed [15].

In Ref. [21], Ottaviani *et al.* theoretically studied the atom-light interaction in the spontaneous Raman process (SRP) beyond the adiabatic approximation. Compared with the SRP in the adiabatic approximation, the detuning between the frequency of the light and the atom is smaller in SRP beyond the adiabatic approximation. Due to this smaller detuning, the unwanted excitation among nearby levels can be avoided. The problem with or without adiabatic approximation emerges in the study of an EIT system [22,23]. In most previous studies on quantum memory based on EIT, the key assumption has been adiabatic approximation, which requests the atomic medium to be optically dense, and sets a limit to the switching time of the control field. It is assumed that the adiabaticity conditions are satisfied, the dark-state polariton is shape preserving during its propagation, and thus the retrieved photons resemble the probe photons [24,25]. However, the adiabaticity conditions cannot always be fulfilled in practice [11,22,26–28]. For example, in the very important case of short probe pulse memory [11,26,29], the adiabaticity conditions can hardly hold due to the restrictions of the EIT bandwidth, and geometrical size of an atomic medium. Therefore, to achieve high-quality storage in such a case, we actually need a nonadiabatic theory especially for the goal of efficiency optimization through setting appropriately experimental parameters. Excellent results for such a goal were presented in [30,31]. In particular, to optimize the quantum memory efficiency, one can use the theoretical method in [31], through using a carefully designed control field. To make it technically easier for practical application, it is very desirable to study the problem on how to achieve the same efficiency by applying easily shaped control fields. In this paper, we study this problem.

We shall study the total storage efficiency in an EIT medium, with and without adiabatic approximation, and derive analytical expressions for that total storage efficiency. According to these formulas, we perform numerical simulations with an easily shaped control field which has been widely applied in existing experiments. Our maximum value of storage

*xbwang@mail.tsinghua.edu.cn

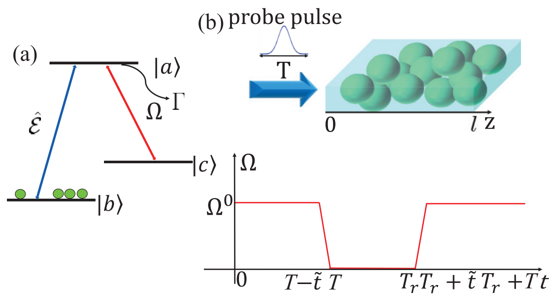

FIG. 1. (a) Λ-type EIT system coupled resonantly to a strong classical control field Ω and a weak probe field $\hat{\mathcal{E}}$. The decay rate of excited state $|a\rangle$ is Γ. (b) Process of quantum memory. The strength of the control field changes with time, $\tilde{t}$ represents the switching time and Ω^0 is the maximum Rabi frequency. The storage time of a probe pulse in the process is $T_r - T$.

efficiency is quite close to the optimal results in literature [31], but we do not need any complicated-design control field. Our numerical simulation results are in good agreement with the existing experiments [11,32]. Furthermore, we find that the difference between adiabatic and nonadiabatic storage efficiency is quite evident when we store short probe pulses; hence, the nonadiabatic corrections cannot be neglected. Then, by introducing a quasiparticle picture [24,25], we study how the nonadiabatic corrections change with experimental parameters.

The rest of this paper is organized as follows. In Sec. II, combining with the Maxwell-Bloch equations for the quantum probe field and classical control field in an atomic EIT medium, we derive the analytical expression for the total number of retrieved probe photons. Then, in Sec. III, the total storage efficiency is achieved with and without adiabatic approximation. By numerical simulation in Sec. IV, we analyze how the adiabatic and nonadiabatic storage efficiencies change with different system parameters. Moreover, in Sec. V, we also discuss the difference between adiabatic and nonadiabatic storage efficiency under various strengths and switching times of the control field. Finally, we give a conclusion in Sec. VI.

II. THEORETICAL MODEL

Following [31], we begin our study with a typical EIT system as illustrated in Fig. 1. A beam of weak probe field and a beam of strong control field propagate through an atomic ensemble in the z direction. The atomic ensemble contains N Λ-type atoms with two lower metastable states $|b\rangle$ and $|c\rangle$, and one excited state $|a\rangle$, whose decay rate is Γ. The probe field described by the operator $\hat{\mathcal{E}}(z,t)$ in the slowly varying envelope approximation, couples resonantly the transition between state $|b\rangle$ and $|a\rangle$. The excited state $|a\rangle$ is furthermore coupled to state $|c\rangle$ via the strong control field with slowly varying, real Rabi frequency $\Omega(t - z/c)$. Here, we assume that the probe field and control field are uniform in the transverse direction. In the Heisenberg picture, the equations of motion can be written as [31]

$$(\partial_t + c\partial_z)\hat{\mathcal{E}}(z,t) = igN\hat{\sigma}_{ba}(z,t), \tag{1}$$

$$\partial_t\hat{\sigma}_{ba}(z,t) = -\gamma_{ba}\hat{\sigma}_{ba}(z,t) + ig\hat{\mathcal{E}}(z,t) + i\Omega\hat{\sigma}_{bc}(z,t), \tag{2}$$

$$\partial_t\hat{\sigma}_{bc}(z,t) = i\Omega^*\hat{\sigma}_{ba}(z,t), \tag{3}$$

where $\hat{\sigma}_{\mu\nu} = \frac{1}{N_z}\sum_{j=1}^{N_z}\hat{\sigma}_{\mu\nu}^{(j)}e^{-i\omega_{\mu\nu}t+i\frac{\omega_{\mu\nu}}{c}z}$ $(\mu,\nu = a,b,c)$ is the slowly varying, collective atomic operator, N_z is the number of atoms in a small region at position z, g denotes the coupling strength between the probe field and an atom, and c is the speed of light in the vacuum. Dephasing rate of $\hat{\sigma}_{ba}$ is described by γ_{ba}, and $\gamma_{ba} = \Gamma/2$. We disregard γ_{bc} because the transition between $|b\rangle$ and $|c\rangle$ is not dipole allowed [10,31].

In the process of optical quantum memory based on EIT, all atoms are initially in the ground state $|b\rangle$, a probe pulse whose duration is T enters the atomic ensemble at time $t = 0$, and is fully stored at time T, as the intensity of control field decreases to zero. At any time $t = T_r (T_r > T)$, corresponding to the storage time $T_r - T$, with the control field being switched on, the probe pulse is released from the atomic ensemble, and we can retrieve the information we have stored. To describe the process mathematically, we write the following initial and boundary conditions, $\hat{\mathcal{E}}_{\text{in}}(t) = \hat{\mathcal{E}}(0,t)(0 \leqslant t \leqslant T)$, $\hat{\mathcal{E}}(0,t) = 0(t > T)$, $\hat{\mathcal{E}}_{\text{out}}(t) = \hat{\mathcal{E}}(l,t)$ (l is the length of an atomic ensemble in the z direction), and $\hat{\sigma}_{ba}(z,0) = 0$, $\hat{\sigma}_{bc}(z,0) = 0$. The total storage efficiency is defined as [10,31]

$$\eta = \frac{\text{number of retrieved photons}}{\text{number of incoming photons}} = \frac{n_{\text{out}}}{n_{\text{in}}} = \frac{\int_{T_r}^{\infty}\langle\hat{\mathcal{E}}_{\text{out}}^{+}\hat{\mathcal{E}}_{\text{out}}\rangle dt}{\int_0^T\langle\hat{\mathcal{E}}_{\text{in}}^{+}\hat{\mathcal{E}}_{\text{in}}\rangle dt}. \tag{4}$$

For our interests in studying the storage efficiency, it is quite important to get the analytical expression of n_{out} given n_{in}. Referring to the computation method in [22] and [31], we transform our system into a comoving frame by changing the variables $t' = t - z/c$ and $\xi = z/l$, and make the Laplace transformation to map ξ space to s space, $\hat{\mathcal{E}}(\xi,t') \to \hat{E}(s,t')$, $\hat{\sigma}_{ba}(\xi,t') \to \hat{P}(s,t')$, and $\hat{\sigma}_{bc}(\xi,t') \to \hat{S}(s,t')$. We find

$$\begin{aligned}\int_{T_r-\frac{l}{c}}^{\infty}&\langle\hat{E}^{+}(s'^{*},t')\hat{E}(s,t')\rangle dt' \\ &= -\frac{l}{c}\frac{d}{2}\frac{2N}{2ss'^{*} + s'^{*}d + sd}[\langle\hat{P}^{+}(s'^{*},t')\hat{P}(s,t')\rangle \\ &\quad + \langle\hat{S}^{+}(s'^{*},t')\hat{S}(s,t')\rangle]_{T_r-\frac{l}{c}}^{\infty}.\end{aligned} \tag{5}$$

Here, $d = g^2Nl/\gamma_{ba}c$ is the optical depth of the medium. Combining this with $\lim_{t'\to\infty}\hat{P}(s,t') = 0$, $\lim_{t'\to\infty}\hat{S}(s,t') = 0$, and taking inverse Laplace transformation for Eq. (5), we get

$$\begin{aligned}n_{\text{out}} &= \int_{Tr}^{\infty}dt\langle\hat{\mathcal{E}}_{\text{out}}^{+}\hat{\mathcal{E}}_{\text{out}}\rangle \\ &= \int_{T_r-\frac{l}{c}}^{\infty}dt'\langle\hat{\mathcal{E}}^{+}(1,t')\hat{\mathcal{E}}(1,t')\rangle \\ &= \int_0^1 d\xi\int_0^1 d\xi'\frac{Nl}{c}\frac{d}{2}e^{-d}e^{\frac{d}{2}(\xi+\xi')}I_0[d\sqrt{(1-\xi)(1-\xi')}] \\ &\quad\times\left\langle\hat{\sigma}_{cb}\left(\xi',T_r - \frac{l}{c}\right)\hat{\sigma}_{bc}\left(\xi,T_r - \frac{l}{c}\right)\right\rangle,\end{aligned} \tag{6}$$

where I_0 is a zeroth-order modified Bessel function. From Eq. (6), we note that the photon number of the retrieved probe pulse only depends on $\hat{\sigma}_{bc}(\xi,T_r - \frac{l}{c})$, which describes the collective atomic coherence at the moment of switching on the control field. And it also shows coincidence with the physical mechanism of EIT quantum memory, as the dark state provides a probability to transfer the photonic state to the collective atomic state mutually, by changing the intensity of the control field.

III. STORAGE EFFICIENCY

In the previous section, we found that the total storage efficiency is dependent on the collective atomic coherence at the moment of retrieving. Here we will first study their relationship both adiabatically and nonadiabatically. And then, we will present the analytical expressions of the storage efficiency in both cases.

A. Adiabatic storage efficiency

Under the adiabatic approximation, we can eliminate $\hat{\sigma}_{ba}$ in Eq. (2) and obtain the relation $\hat{\sigma}_{bc} = -g\hat{\mathcal{E}}/\Omega$. By using Laplace transformation as before, we get the equation for $\hat{S}(\hat{\sigma}_{bc})$ in s space:

$$\partial_{t'}\hat{S}(s,t') + M(t')\hat{S}(s,t') = N(t'), \tag{7}$$

$$M(t') = \frac{c\Omega^2(t')s}{g^2Nl}, \tag{8}$$

$$N(t') = -\frac{c\Omega(t')}{gNl}\hat{\mathcal{E}}(0,t'). \tag{9}$$

Equation (7) is a first-order nonhomogeneous nonlinear differential equation, and we can solve it analytically and find its solution,

$$\hat{S}(s,t') = -\frac{g}{\gamma_{ba}d}\int_0^{t'} e^{\frac{s}{d}\kappa(t'',t')}\Omega(t'')\hat{\mathcal{E}}(0,t'')dt'', \tag{10}$$

$$\kappa(t'',t') = \frac{1}{\gamma_{ba}}\int_{t'}^{t''}\Omega^2(\tau)d\tau. \tag{11}$$

After taking the inverse Laplace transformation, the analytical expression of $\hat{\sigma}_{bc}$ is

$$\hat{\sigma}_{bc}(\xi,t') = -\frac{g}{\Omega(t_p')}\hat{\mathcal{E}}(0,t_p'), \tag{12}$$

where t_p' satisfies the relation $\int_0^{t_p'}\Omega^2(\tau)d\tau = \int_0^{t'}\Omega^2(\tau)d\tau - \gamma_{ba}d\xi$. When a probe pulse starts to propagate in the medium with a reduced group velocity $v_g \sim \frac{c\Omega^2(\tau)}{g^2N}$, at time t_p', it will arrive at position ξ at time t'. Substituting Eq. (12) into Eq. (6), we can write the photon number of the retrieved probe pulse as

$$n_{\text{out}} = \int_0^1 d\xi\int_0^1 d\xi' k_d(\xi,\xi')\frac{\gamma_{ba}d}{\Omega(t_p')\Omega(t_p'')}\langle\hat{\mathcal{E}}^+(0,t_p'')\hat{\mathcal{E}}(0,t_p')\rangle, \tag{13}$$

$$k_d(\xi,\xi') = \frac{d}{2}e^{-d}e^{\frac{d}{2}(\xi+\xi')}I_0[d\sqrt{(1-\xi)(1-\xi')}]. \tag{14}$$

Given the widely employed temporal Gaussian probe pulse [15,32], the total storage efficiency with the adiabatic approximation can be furthermore expressed as

$$\eta_a = \frac{2}{\Delta t}\sqrt{\frac{ln2}{\pi}}\int_0^1 d\xi\int_0^1 d\xi' k_d(\xi,\xi')\frac{\gamma_{ba}d}{\Omega(t_p')\Omega(t_p'')} \times e^{-\frac{2ln2(t_p''-t_0)^2}{\Delta t^2}}e^{-\frac{2ln2(t_p'-t_0)^2}{\Delta t^2}}. \tag{15}$$

Here Δt is the FWHM temporal duration of the probe pulse, t_0 is the position of the probe pulse peak.

B. Nonadiabatic storage efficiency

In the nonadiabatic case, the photon number of a probe pulse is much smaller than the number of atoms. Almost all the atoms are in the ground state $|b\rangle$, and furthermore, the excitation rate of the atoms stimulated to state $|a\rangle$ is much smaller than the decay rate γ_{ba}. Consequently, the time derivative term $\partial_t\hat{\sigma}_{ba}$ in Eq. (2) can be neglected. Then, by adopting the same procedure used in the last section, we obtain

$$\hat{S}(s,t') = -\sqrt{\frac{dc}{\gamma_{ba}lN}}\int_0^{t'}\frac{1}{s+d}e^{\frac{s}{s+d}\kappa(t'',t')}\Omega(t'')\hat{\mathcal{E}}(0,t'')dt''. \tag{16}$$

Note that in the perfect adiabaticity condition $d \to \infty$, as mentioned below, one may easily find that the expression in Eq. (16) can change to Eq. (10). After taking the inverse Laplace transformation, we get

$$\hat{\sigma}_{bc}(\xi,t') = -\sqrt{\frac{dc}{\gamma_{ba}lN}}\int_0^{t'} e^{\kappa(t'',t')}\Omega(t'')e^{-d\xi} \times I_0[\sqrt{4d\kappa(t',t'')\xi}]\hat{\mathcal{E}}(0,t'')dt''. \tag{17}$$

Substituting the above equation into Eq. (6), the nonadiabatic result for the number of retrieved photons is

$$n_{\text{out}} = \int_0^1 d\xi\int_0^1 d\xi' k_{dd}(\xi,\xi')\int_0^{T_r-\frac{l}{c}}dt'\int_0^{T_r-\frac{l}{c}}dt'' \times e^{-\kappa(T_r-\frac{l}{c},t')}e^{-\kappa(T_r-\frac{l}{c},t'')}\Omega(t')\Omega(t'') \times I_0\left[\sqrt{4d\kappa\left(T_r-\frac{l}{c},t'\right)\xi'}\right]I_0\left[\sqrt{4d\kappa\left(T_r-\frac{l}{c},t''\right)\xi}\right] \times\langle\hat{\mathcal{E}}^+(0,t')\hat{\mathcal{E}}(0,t'')\rangle, \tag{18}$$

$$k_{dd}(\xi,\xi') = \frac{d^2}{2\gamma_{ba}}e^{-d}e^{-\frac{d}{2}(\xi+\xi')}I_0[d\sqrt{(1-\xi)(1-\xi')}]. \tag{19}$$

Considering a temporal Gaussian probe pulse as in the last section, we can also write the total storage efficiency without adiabatic approximation as

$$\eta_{na} = \frac{2}{\Delta t}\sqrt{\frac{ln2}{\pi}}\int_0^1 d\xi\int_0^1 d\xi' k_{dd}(\xi,\xi')\int_0^{T_r-\frac{l}{c}}dt' \times\int_0^{T_r-\frac{l}{c}}dt'' e^{-\kappa(T_r-\frac{l}{c},t')}e^{-\kappa(T_r-\frac{l}{c},t'')}\Omega(t')\Omega(t'') \times I_0\left[\sqrt{4d\kappa\left(T_r-\frac{l}{c},t'\right)\xi'}\right]I_0\left[\sqrt{4d\kappa\left(T_r-\frac{l}{c},t''\right)\xi}\right] \times e^{-\frac{2ln2(t'-t_0)^2}{\Delta t^2}}e^{-\frac{2ln2(t''-t_0)^2}{\Delta t^2}}. \tag{20}$$

TABLE I. Theoretical and experimental storage efficiencies. Ref. [11] shows the storage experiment for a 100-ns short probe pulse, while Ref. [32] shows the experiment for a 4.5-μs long probe pulse. The optical depths of the atomic media in these two experiments are 4 and 156, respectively. η: the experimental results reported in the literature. η_a and η_{na}: the theoretical simulation results with or without adiabatic approximation, respectively.

Expt.	η	η_a	η_{na}
Ref. [11]	8.3%	6.75%	9.03%
Ref. [32]	69%	71.9%	70.58%

TABLE II. Maximum storage efficiencies and the corresponding optimum optical depths for different intensities of control field in Fig. 2. Ω^0: the strength of control field. d_o^a and d_o^{na}: the optimum optical depths with or without adiabatic approximation. η_{max}^a and η_{max}^{na}: the corresponding maximum storage efficiencies with or without adiabatic approximation, respectively.

Ω^0	d_o^a	η_{max}^a	d_o^{na}	η_{max}^{na}
0.8Γ	2.6	49.07%	4.2	24.3%
1.1Γ	5	60.59%	7	35.46%
1.3Γ	7	65.93%	9	42.23%

IV. MEMORY EFFICIENCY OPTIMIZATION

Referring to the research on optical storage experiments in [11] and [32], we apply our results in earlier sections. The good agreement between our theory and experiments can be found in Table I. We also show how they change when we store a short and a long temporal Gaussian probe pulse under the parameters set as follows. The corresponding duration of the short and long probe pulses are 100 ns and 4.5 μs, respectively. And the switching time of control field is 30 ns. Simulation results are shown in Figs. 2(a)–2(f) for three different intensities of control field, i.e., $\Omega^0 = 0.8\Gamma, 1.1\Gamma, 1.3\Gamma$.

Under different strengths of control field, we can always find an optimum optical depth to achieve a maximum storage efficiency. Moreover, as the control field gets stronger, both the maximum storage efficiency and the corresponding optimum optical depth get larger. In the range of our chosen parameters, this phenomenon can be shown more evidently from the simulation results in the short probe pulse case, which are listed in Table II, and explained as follows. On the one hand, the EIT bandwidth is proportional to $|\Omega|^2/\sqrt{d}$, so a larger d results in a narrower EIT window, while a larger Ω makes it wider. On the other hand, d is the absorbance of the atomic ensemble, therefore a larger d can lead to the storage efficiency rising. These two contributions generate the above phenomenon.

By changing the intensity of the control field, the transformation between photonic states and collective atomic states can be achieved. Thus, the switching time, which determines how the control-field intensity changes, can also affect the storage efficiency. The simulation results, which correspond to the case when we store a 100-ns short probe pulse, are shown in Figs. 3(a)–3(c). The control-field intensities are 0.8Γ, 1.1Γ, and 1.3Γ, respectively. And the optical depths are the same as the optimum optical depths in Table II. Under different strengths of control field and optical depths, one can also find an optimum switching time and a corresponding maximum storage efficiency, see Table III. The maximum storage efficiencies are close to the efficiencies in Table II, as we have already utilized an excellent switching time to achieve the results in Table II.

Comparing our simulation results with the storage efficiency, which is less than 10% [11,26,29], obtained by the current experiments for a short probe pulse, we find that our simulated maximum storage efficiency is quite good. And it is noteworthy that we adopt the control field whose shape is as

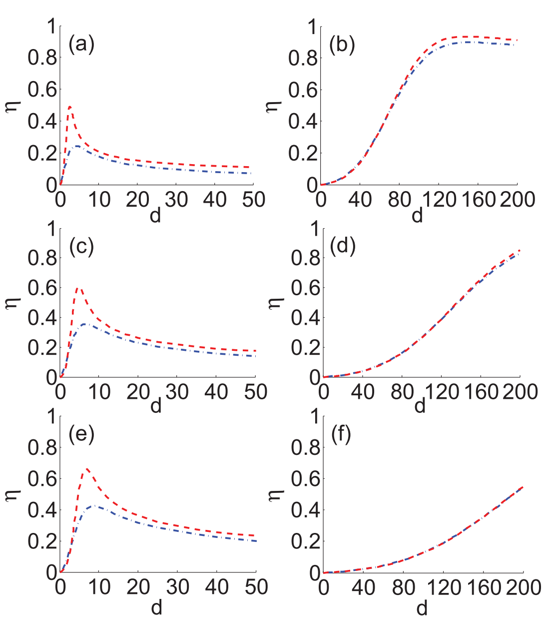

FIG. 2. Numerical results for the total storage efficiency. Dashed line: adiabatic result. Dash-dotted line: nonadiabatic result. η: total storage efficiency. d: optical depth. (a), (c), and (e): results for short probe pulse of duration $T = 100$ ns and FWHM $\Delta t = 30$ ns; (b), (d), and (f): results of long probe pulse $T = 4.5$ μs, FWHM $\Delta t = 1.5$ μs. The strengths of control fields are (a) and (b) $\Omega^0 = 0.8\Gamma$, (c) and (d) $\Omega^0 = 1.1\Gamma$, (e) and (f) $\Omega^0 = 1.3\Gamma$, the switching time is 30 ns. The decay rate γ_{ba} is set as $\pi \times 6 \times 10^6$ Hz.

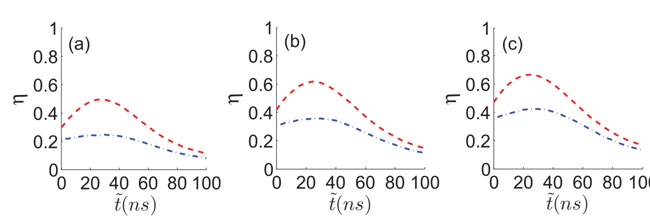

FIG. 3. Numerical results for the total storage efficiency. Dashed line: adiabatic result. Dash-dotted line: nonadiabatic result. η: total storage efficiency. $\tilde{t}$: switching time of control field. The strengths of the control fields are (a) $\Omega^0 = 0.8\Gamma$, (b) $\Omega^0 = 1.1\Gamma$, and (c) $\Omega^0 = 1.3\Gamma$; the optical depths corresponding to the adiabatic results are (a) $d = 2.6$, (b) $d = 5$, and (c) $d = 7$; optical depths for the nonadiabatic results are (a) $d = 4.2$, (b) $d = 7$, and (c) $d = 9$. The duration of the short probe pulse $T = 100$ ns and FWHM $\Delta t = 30$ ns. The decay rate γ_{ba} is $\pi \times 6 \times 10^6$ Hz.

TABLE III. Maximum storage efficiencies and the corresponding optimum switching times for different control-field intensities and optimum optical depths in Fig. 3. Ω^0: the strength of control field. d_o^{a} and d_o^{na}: the corresponding optimum optical depths with or without adiabatic approximation in Table II. $\tilde{t}_0^{\mathrm{a}}$ and $\tilde{t}_0^{\mathrm{na}}$: the optimum switching time with or without adiabatic approximation, respectively. $\eta_{\max}^{\mathrm{a}}$ and $\eta_{\max}^{\mathrm{na}}$: the corresponding maximum storage efficiencies with or without adiabatic approximation.

Ω^0	d_o^{a}	$\tilde{t}_o^{\mathrm{a}}$ (ns)	$\eta_{\max}^{\mathrm{a}}$	d_o^{na}	$\tilde{t}_o^{\mathrm{na}}$ (ns)	$\eta_{\max}^{\mathrm{na}}$
0.8Γ	2.6	25	49.1%	4.2	30	24.3%
1.1Γ	5	25	61.49%	7	25	35.52%
1.3Γ	7	25	66.98%	9	30	42.23%

illustrated in Fig. 1(b) to complete the above simulation. This kind of operation about the control field is easy in manipulation and widely applied in experiments [32,33]. Though our proposed control field is very simple, our results are close to the theoretical results obtained from the optimal control pulses presented in [30,31]. For example, when $d_o^{\mathrm{na}} = 9$, the maximum nonadiabatic storage efficiency $\eta_{\max}^{\mathrm{na}} = 42.23\%$, while the corresponding maximum efficiency reported in the literature equals 46%.

By comparing the results shown in Figs. 2(a)–2(f), we can also find that the optimum d for the storage of a 4.5- μs probe pulse is much larger than that for the storage of a 100-ns probe pulse. There are two requirements in EIT optical storage: (i) the spectrum of the probe pulse must fit within the transparency window; (ii) the probe pulse must fit geometrically within the EIT medium, since the spatial extent of the probe pulse can be compressed as a result of the low group velocity [3]. One can conclude that with the aim of accomplishing high storage efficiency under the general strength of the control field, the optimum d needed for storing short probe pulses is much lower than that for long probe pulses. As shown in Figs. 2(a)–2(f), the difference between adiabatic and nonadiabatic storage efficiency is much evident when we store a short probe pulse, but microsized for the long probe pulse case. Considering the adiabaticity condition addressed in Ref. [25], the storage and retrieval process of the photon pulse can work adiabatically with two requirements satisfied simultaneously:

$$l \ll \sqrt{d}L_p, \tilde{t} > \frac{\gamma_{ba}{\Omega^0}^2}{g^2N(g^2N+{\Omega^0}^2)}, \tag{21}$$

where L_p denotes the initial spatial pulse length in the medium. Since the spatial pulse length is smaller or comparable to the size of the atomic medium, the first inequality in Eq. (21) can be satisfied when $d \gg 1$. In other words, it is hard to be adiabatic when the atomic medium is not optically dense [25]. Given our chosen parameters in Figs. 2 and 3, when we store a short probe pulse, the first inequality in Eq. (21) does not hold. For example, in the short-pulse memory, the length of the atomic medium l is 3×10^{-4} m [17], but $\sqrt{d}L_p$ is just 5.8×10^{-4} m, when the optical depth d is 5 and Ω^0 equals 0.8Γ. Thus, the nonadiabatic terms cannot be neglected in this nonadiabatic case, therefore the EIT quantum memory beyond adiabatic approximation is deserved to be studied much further.

V. NONADIABATIC CORRECTIONS

In this section, we shall study quantum memory without adiabatic approximation. The difference in the storage efficiency between the adiabatic and nonadiabatic cases will be presented below. The quasiparticle picture is used and two new quantum operators $\hat{\Psi}(z,t)$ and $\hat{\Phi}(z,t)$ [24,25] are applied,

$$\hat{\Psi} = \cos\theta\hat{\mathcal{E}} - \sin\theta\sqrt{N}\hat{\sigma}_{bc}, \tag{22}$$

$$\hat{\Phi} = \sin\theta\hat{\mathcal{E}} + \cos\theta\sqrt{N}\hat{\sigma}_{bc}, \tag{23}$$

where $\tan\theta = g\sqrt{N}/\Omega$. By substituting the relations above into Eq. (1)–(3), one can obtain the equations of motion for the two operators $\hat{\Psi}$ and $\hat{\Phi}$,

$$\partial_t\hat{\Psi} + c\cos^2\theta\partial_z\hat{\Psi} = -\dot{\theta}\hat{\Phi} - c\sin\theta\cos\theta\partial_z\hat{\Phi}, \tag{24}$$

$$\hat{\Phi} = \frac{\gamma_{ba}\cos\theta}{\Omega^2}(\cos\theta\dot{\theta}\hat{\Psi} + \sin\theta\partial_t\hat{\Psi} + \sin\theta\dot{\theta}\hat{\Phi} - \cos\theta\partial_t\hat{\Phi}). \tag{25}$$

By applying the Fourier transforms as $\hat{\Psi}(z,t) = \int\hat{\Psi}(k,t)e^{-ikz}dk$ and $\hat{\Phi}(z,t) = \int\hat{\Phi}(k,t)e^{-ikz}dk$ in the adiabatic limit, one can find $\hat{\Phi} = 0$ and $\partial_t\hat{\Psi}(k,t) = ikc\cos^2\theta\hat{\Psi}(k,t)$. However, in the nonadiabatic limit, considering the lowest order nonadiabatic corrections, we can obtain Eqs. (24) and (25) in the k space as

$$\partial_t\hat{\Psi}(k,t) - ikc\cos^2\theta\hat{\Psi}(k,t) = -\dot{\theta}\hat{\Phi}(k,t) + ikc\sin\theta\cos\theta\hat{\Phi}(k,t), \tag{26}$$

$$\hat{\Phi}(k,t) = \frac{\gamma_{ba}\cos\theta}{\Omega^2}[\cos\theta\dot{\theta}\hat{\Psi}(k,\ t) + ikc\sin\theta\cos^2\theta\hat{\Psi}(k,t)]. \tag{27}$$

By substituting Eq. (27) into Eq. (26), we finally obtain the dark state polariton beyond adiabatic approximation as follows:

$$\hat{\Psi}(k,t) = \hat{\Psi}(k,0)e^{\int_0^t ikv_g(t')dt'}e^{-\int_0^t[A(t')+B(t')]dt'}. \tag{28}$$

Here, $v_g = c\cos^2\theta$ is the group velocity of a probe pulse in an atomic medium, $A(t) = \gamma_{ba}\cos^2\theta\dot{\theta}^2/\Omega^2$, and $B(t) = \gamma_{ba}k^2c^2\cos^4\theta\sin^2\theta/\Omega^2$. From Eq. (28), we find that the integral term $\int_0^t[A(t')+B(t')]dt'$ brings about the nonadiabatic correction. When it equals zero or is small compared to unity (adiabatic approximation), the dark state polariton $\hat{\Psi}(k,t) = \hat{\Psi}(k,0)e^{\int_0^t ikv_g(t')dt'}$. However, if the integral term is not small enough, one cannot neglect it, and the nonadiabatic correction needs to be considered in this scenario. Moreover, it is easy to find that the integral term can be determined by the control field Ω; different control fields yield different nonadiabatic corrections. Considering the control field as illustrated in Fig. 1(b), we just need to calculate the integral $\int_0^t[A(t')+B(t')]dt'$ with the upper limit t as T. Hence, we get the nonadiabatic correction function

$$\begin{aligned} f(\Omega^0,\tilde{t}) &= \int_0^T [A(t') + B(t')]dt' \\ &= \frac{\gamma_{ba}\Omega^{0^2} g^2 N(T-\tilde{t})}{4T^2(g^2N+\Omega^{0^2})^3} + \frac{\gamma_{ba}\Omega^{0^2}}{4\tilde{t}(g^2N+\Omega^{0^2})^2} + \frac{3\gamma_{ba}\Omega^{0^2}}{8\tilde{t}g^2N(g^2N+\Omega^{0^2})} + \frac{3\gamma_{ba}\Omega^0}{8\tilde{t}g^2Ng\sqrt{N}}\arctan\left(\frac{\Omega^0}{g\sqrt{N}}\right) \\ &+ \frac{g^2N\Omega^{0^4}\tilde{t}}{4\gamma_{ba}d}\left[\frac{1}{(g^2N+\Omega^{0^2})^2} - 5g^2N\left(-\frac{1}{\Omega^{0^2}(g^2N+\Omega^{0^2})^2} + \frac{3g^2N}{\Omega^{0^2}}\left\{\frac{1}{4g^2N(g^2N+\Omega^{0^2})^2} + \frac{1}{4g^2N}\right.\right.\right. \\ &\left.\left.\left.\times\left[-\frac{1}{2\Omega^{0^2}(g^2N+\Omega^{0^2})} + \frac{1}{2\Omega^{0^3}g\sqrt{N}}\arctan\left(\frac{\Omega^0}{g\sqrt{N}}\right)\right]\right\}\right)\right]. \end{aligned} \tag{29}$$

From the simulation results in Fig. 4, we find that with a larger intensity and a shorter switching time of the control field, a larger nonadiabatic correction f can be obtained. In our discussion, the optical depth of the medium is set as 7. Considering the adiabaticity condition of Eq. (21) addressed in the last section, for our case, the first requirement is broken, and the second one can be satisfied. So in our discussion, the storage and retrieval process of the photon pulse is nonadiabatic. However, in comparison, we also study for the 4.5-μs long probe pulse. The optical depth is 156, and thus the adiabaticity condition $l \ll \sqrt{d}L_p$ is satisfied. In this case, the nonadiabatic corrections are always smaller than unity, no matter how fast the control field is switched, as shown in Fig. 4. This point has been carefully studied in Ref. [23]. And our results with the 4.5-μs long probe pulse show good agreement with the results reported in Ref. [23].

To illustrate the difference in the storage with or without adiabatic approximation, we define $\Delta\eta = \eta_a - \eta_{na}$, which denotes the difference in the storage efficiency of quantum memory with or without adiabatic approximation. The relation between $\Delta\eta$ and f has been addressed in Fig. 5. For our chosen parameters, the simulation results show the positive relation between $\Delta\eta$ and f. Thus, $\Delta\eta$ can be used to reflect the difference between the adiabatic and nonadiabatic cases.

In Fig. 6, we show how $\Delta\eta$ changes with switching time $\tilde{t}$. The control fields with different strengths are provided. In our scenario, when the switching time is larger, $\Delta\eta$ always converges to the value which is much smaller than unity. As mentioned before, storage and retrieval of a photon pulse can be seen as an adiabatic process when the two requirements are satisfied. When we store a 100-ns probe pulse, the first adiabaticity condition $l \ll \sqrt{d}L_p$ is broken, and this process cannot be seen as an adiabatic process. However, when $\tilde{t} > 80$ ns is chosen in our simulation, the nonadiabatic storage efficiency is much closer to the adiabatic storage efficiency, i.e., $\Delta\eta \sim 1\%$. This result reflects that although the first adiabaticity condition is broken, the effect of adiabatic approximation can be nearly achieved by increasing the switching time of the control field.

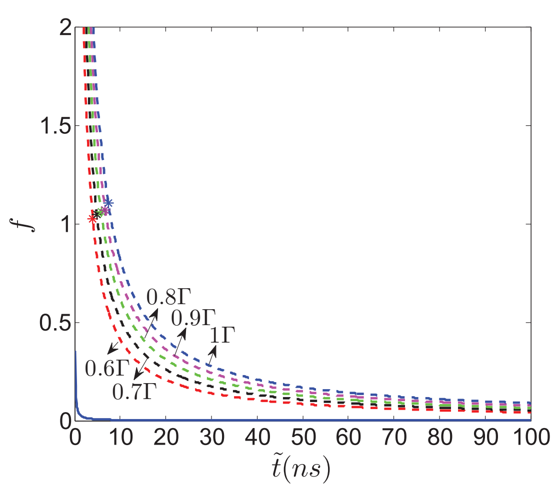

FIG. 4. Numerical results for the nonadiabatic correction function f. Dashed lines: results for 100-ns short probe pulse, under different strengths of control field $\Omega^0 = 0.6\Gamma, 0.7\Gamma, 0.8\Gamma, 0.9\Gamma$, and 1Γ, respectively. The optical depth d is 7. The point on the dashed line corresponds to the adiabaticity condition $\tilde{t} > \gamma_{ba}\Omega^{0^2}/g^2N(g^2N + \Omega^{0^2})$. Solid line: result for 4.5-μs long probe pulse. The intensity of control field Ω^0 is 1.1Γ and the optical depth d is 156.

VI. CONCLUSIONS

In conclusion, in this article, we have presented a detailed analysis of light storage efficiency in an EIT-driven Λ-type atomic ensemble. We have derived the analytical expressions of the total storage efficiency with and without adiabatic

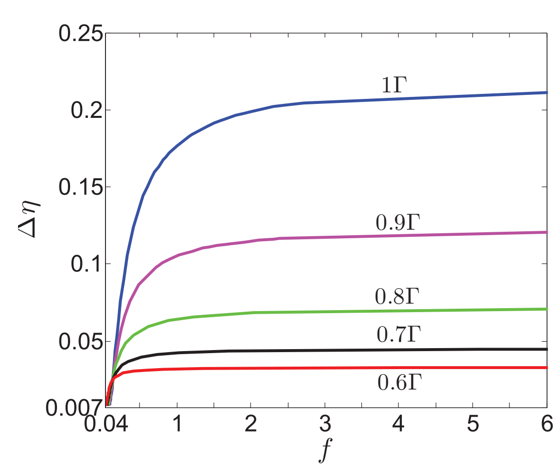

FIG. 5. Numerical results for the relation between $\Delta\eta$ and f for different control-field strengths Ω^0. The optical depth d is set as 7, and the duration of probe pulse is 100 ns, FWHM is 30 ns.

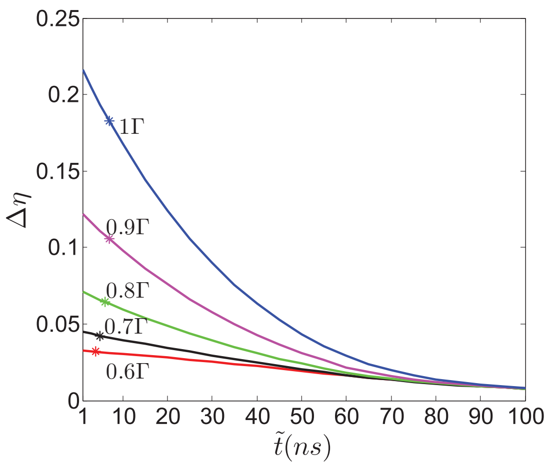

FIG. 6. Difference between adiabatic and nonadiabatic storage efficiency $\Delta\eta$ as a function of switching time $\tilde{t}$ for different control-field strengths Ω^0. The point on the solid line corresponds to the adiabaticity condition. We set the optical depth d of the medium as 7, the duration T of the Gaussian probe pulse as 100 ns and FWHM as 30 ns.

approximation. The influence of systematic parameters on the storage efficiency has been also studied in detail. In particular, we adopt an easily shaped control field in this work. This kind of control field is easier to realize and widely applied in experiments [32,33]. We further optimize the storage efficiency by finding optimum parameters in the very important case of short-pulse memory, which mostly corresponds to a nonadiabatic regime. Our achieved maximum efficiency is rather close to the theoretical limit in Ref. [30,31]. The presented optimization can substantially increase the memory efficiency of ongoing experiments on short-pulse memory.

In addition to atomic ensembles, there are many other systems for light storage, such as a rare-earth-metal ion-doped crystal [34]. We expect our work can be applicable to these solid-state memory experiments. In this paper, we only study the light storage in three-level Λ-type atomic ensembles. It is possible to extend to other systems, e.g., a five-level atomic medium [35]. Fidelity may also be studied in the nonadiabatic regime, because it is an important character of memory in addition to efficiency. We also expect our efforts regarding short-pulse memory can be applied to studies of multimode memory [36,37].

ACKNOWLEDGMENTS

We acknowledge support from Shandong Province, the National High-Tech Program of China Grants No. 2011AA010800 and No. 2011AA010803, and National Natural Science Foundation of China Grants No. 11174177, No. 11474182, and No. 60725416.

[1] M. Fleischhauer, A. Imamoglu, and J. P. Marangos, Rev. Mod. Phys. **77**, 633 (2005).

[2] L.-M. Duan, M. D. Lukin, J. I. Cirac, and P. Zoller, Nature **414**, 413 (2001).

[3] A. I. Lvovsky, B. C. Sanders, and W. Tittel, Nat. Photon. **3**, 706 (2009).

[4] B. Zhao, Y. A. Chen, X. H. Bao, T. Strassel, C. S. Chuu, X. M. Jin, J. Schmiedmayer, Z. S. Yuan, S. Chen, and J. W. Pan, Nat. Phys. **5**, 95 (2009).

[5] Y. O. Dudin, S. D. Jenkins, R. Zhao, D. N. Matsukevich, A. Kuzmich, and T. A. B. Kennedy, Phys. Rev. Lett. **103**, 020505 (2009).

[6] R. Zhao, Y. O. Dudin, S. D. Jenkins, C. J. Campbell, D. N. Matsukevich, T. A. B. Kennedy, and A. Kuzmich, Nat. Phys. **5**, 100 (2009).

[7] X. H. Bao, A. Reingruber, P. Dietrich, J. Rui, A. Dück, T. Strassel, L. Li, N. L. Liu, B. Zhao, and J. W. Pan, Nat. Phys. **8**, 517 (2012).

[8] Y. W. Cho and Y. H. Kim, Opt. Express **18**, 25786 (2010).

[9] A. K. Patnaik, F. L. Kien, and K. Hakuta, Phys. Rev. A **69**, 035803 (2004).

[10] A. V. Gorshkov, A. André, M. D. Lukin, and A. S. Sørensen, Phys. Rev. A **76**, 033804 (2007).

[11] Z. X. Xu, Y. L. Wu, L. Tian, L. R. Chen, Z. Y. Zhang, Z. H. Yan, S. J. Li, H. Wang, C. D. Xie, and K. C. Peng, Phys. Rev. Lett. **111**, 240503 (2013).

[12] J. Rui, Y. Jiang, S. J. Yang, B. Zhao, X. H. Bao, and J. W. Pan, Phys. Rev. Lett. **115**, 133002 (2015).

[13] A. Feizpour, G. Dmochowski, and A. M. Steinberg, Phys. Rev. A **93**, 013834 (2016).

[14] G. Dmochowski, A. Feizpour, M. Hallaji, C. Zhuang, A. Hayat, and A. M. Steinberg, Phys. Rev. Lett. **116**, 173002 (2016).

[15] K. F. Reim, J. Nunn, V. O. Lorenz, B. J. Sussman, K. C. Lee, N. K. Langford, D. Jaksch, and I. A. Walmsley, Nat. Photon. **4**, 218 (2010).

[16] H. de Riedmatten, Nat. Photon. **4**, 206 (2010).

[17] L. V. Hau, S. E. Harris, Z. Dutton, and C. H. Behroozi, Nature **397**, 594 (1999).

[18] C. Ottaviani, S. Rebić, D. Vitali, and P. Tombesi, Phys. Rev. A **73**, 010301(R) (2006).

[19] S. Rebić, C. Ottaviani, G. Di Giuseppe, D. Vitali, P. Tombesi, Phys. Rev. A **74**, 032301 (2006).

[20] A. Feizpour, M. Hallaji, G. Dmochowski, and A. M. Steinberg, Nat. Phys. **11**, 905 (2015).

[21] C. Ottaviani, C. Simon, H. de Riedmatten, M. Afzelius, B. Lauritzen, N. Sangouard, and N. Gisin, Phys. Rev. A **79**, 063828 (2009).

[22] Y.-L. Chuang, I. A. Yu, and R.-K. Lee, Phys. Rev. A **91**, 063818 (2015).

[23] A. B. Matsko, Y. V. Rostovtsev, O. Kocharovskaya, A. S. Zibrov, and M. O. Scully, Phys. Rev. A **64**, 043809 (2001).

[24] M. Fleischhauer and M. D. Lukin, Phys. Rev. Lett. **84**, 5094 (2000).

[25] M. Fleischhauer and M. D. Lukin, Phys. Rev. A **65**, 022314 (2002).

[26] T. Chanelière, D. N. Matsukevich, S. D. Jenkins, S.-Y. Lan, T. A. B. Kennedy, and A. Kuzmich, Nature **438**, 833 (2005).

[27] D. Akamatsu, Y. Yokoi, M. Arikawa, S. Nagatsuka, T. Tanimura, A. Furusawa, and M. Kozuma, Phys. Rev. Lett. **99**, 153602 (2007).

[28] K. Honda, D. Akamatsu, M. Arikawa, Y. Yokoi, K. Akiba, S. Nagatsuka, T. Tanimura, A. Furusawa, and M. Kozuma, Phys. Rev. Lett. **100**, 093601 (2008).

[29] Y. L. Wu, L. R. Chen, Z. X. Xu, and H. Wang, Opt. Express **22**, 23360 (2014).

[30] A. V. Gorshkov, A. André, M. D. Lukin, and A. S. Sørensen, Phys. Rev. A **76**, 033805 (2007).

[31] A. V. Gorshkov, A. André, M. Fleischhauer, A. S. Sørensen, and M. D. Lukin, Phys. Rev. Lett. **98**, 123601 (2007).

[32] Y.-H. Chen, M.-J. Lee, I.-C. Wang, S. Du, Y.-F. Chen, Y.-C. Chen, and I. A. Yu, Phys. Rev. Lett. **110**, 083601 (2013).

[33] U. Schnorrberger, J. D. Thompson, S. Trotzky, R. Pugatch, N. Davidson, S. Kuhr, and I. Bloch, Phys. Rev. Lett. **103**, 033003 (2009).

[34] D. Schraft, M. Hain, N. Lorenz, and T. Halfmann, Phys. Rev. Lett. **116**, 073602 (2016).

[35] G. Grigoryan, V. Chaltykyan, E. Gazazyan, O. Tikhova, and V. Paturyan, Phys. Rev. A **91**, 023802 (2015).

[36] K. Surmacz, J. Nunn, K. Reim, K. C. Lee, V. O. Lorenz, B. Sussman, I. A. Walmsley, and D. Jaksch, Phys. Rev. A **78**, 033806 (2008).

[37] C. Simon, H. de Riedmatten, M. Afzelius, N. Sangouard, H. Zbinden, and N. Gisin, Phys. Rev. Lett. **98**, 190503 (2007).